Lines, Outlines, and Landmarks: Morphometric Analyses of Leaves of Acer rubrum, Acer saccharinum (Aceraceae) and Their Hybrid

Richard J. Jensen; Kristen M. Ciofani; Lydia C. Miramontes

Taxon, Vol. 51, No. 3. (Aug., 2002), pp. 475-492.

Stable URL:
http://links.jstor.org/sici?sici=0040-0262%28200208%2951%3A3%3C475%3ALOALMA%3E2.0.CO%3B2-0

Taxon is currently published by International Association for Plant Taxonomy (IAPT).

MORPHOLOGY

Lines, outlines, and landmarks: morphometric analyses of leaves of *Acer rubrum*, *Acer saccharinum* (Aceraceae) and their hybrid

Richard J. Jensen, Kristen M. Ciofani & Lydia C. Miramontes

Department of Biology, Saint Mary's College, Notre Dame, Indiana 46556, U.S.A. E-mail: rjensen@saintmarys.edu (author for correspondence); kciofani@hotmail.com, lydiamiramontes@hotmail.com

Quantitative comparisons of leaf morphology for evaluating taxonomic relationships may be conducted by traditional morphometrics, outline analyses, or geometric morphometrics. These approaches were employed for examining relationships among trees of two species of maple, *Acer rubrum* and *A. saccharinum*, and their hybrid (*A.* ×*freemanii*). Leaf samples from six hybrid trees (three each from two accessions) and 40 trees field identified as either species were pressed and dried. Leaf outline and landmark data were captured for each leaf, and linear and angular measures were derived from the landmark configurations. A vector of character means, a mean leaf outline, and a consensus landmark configuration were generated for each tree. Traditional morphological measurements, a single-parameter outline descriptor, elliptic Fourier coefficients of the outlines, and relative warp scores for the landmarks were used to depict relationships among the 46 OTUs. All three data types reveal similar patterns with respect to the two species, and the hybrids are generally intermediate between the two species. The results provide evidence of genetic segregation in one hybrid accession, that several of the field sampled trees are naturally occurring hybrids, and that relative warps analysis can reveal aspects of shape variation not detected by the other analyses.

KEYWORDS: *Acer*, Fourier, geometric morphometrics, hybrids, maple, relative warps.

INTRODUCTION

Plant taxonomists have long recognized the importance of leaf features for identifying taxa. In fact, for some groups of plants, e.g., *Quercus*, *Betula*, leaf characters are considered "the most important" (Stace, 1989). The utility of leaf characters for identifying species of trees is demonstrated by their use in virtually all keys to species of woody plants (e.g., Gleason, 1968; Fernald, 1970; Voss, 1972–1996; Elias, 1980); leaf characters are emphasized because floral features either illustrate little variation (e.g., within sections of *Quercus*) or are available only during the relatively short flowering season for each species. The reliance on leaf characters has led to extensive glossaries for both shape and feature differences (e.g., Hickey, 1973; Woodland, 1997). Unfortunately, these terms typically involve subjective interpretations or represent discrete descriptions of what are really continuous characters.

A number of methods for generating quantitative descriptions of leaf shapes have been found to be quite useful for conducting comparisons of shapes within- and among-species (e.g., Dickinson & al., 1987; White & al., 1988; Jensen, 1990; Ray, 1992; Jensen & al., 1993; McLellan, 1993; Paler & Barrington, 1995; Jensen, 1995; Premoli, 1996; McLellan & Endler, 1998; Rumpunen & Bartish, 2002). The methods employed include those based on relationships among simple linear measurements (e.g., lengths, widths; Jensen & al., 1993; McLellan & Endler, 1998; Rumpunen & Bartish, 2002), single-parameter shape descriptors (e.g., fractal dimension, dissection index; Jensen, 1995; McLellan & Endler, 1998), outline decomposition (e.g., elliptic Fourier analysis; White & al., 1988; Jensen, 1995; Premoli, 1996; McLellan & Endler, 1998; Rumpunen & Bartish, 2002), and various approaches for analyzing landmark configurations [e.g., box truss analysis (Dickinson & al., 1987) and Procrustes (= rotational-fit) analyses (Jensen, 1990; Jensen & al., 1993; Paler & Barrington, 1995)]. Each of these methods has strengths and weaknesses, but all have proven effective for describing variation in, and differentiating among, leaf shapes.

In the late 1980s, the focus for analyzing biological shapes shifted from traditional morphometrics to the newly developed methods of geometric morphometrics (Bookstein, 1991; Rohlf & Marcus, 1993). In fact, Bookstein (1991) proclaimed the existence of a new specialty: morphometrics, the biometry of shape. His view was that the methods of traditional morphometrics, e.g., as espoused by Blackith (1965) and Blackith & Reyment

(1971), were devoid of considerations of the nature of the characters—"all were thrown into the same vortex of canonical analyses and clusterings". A significant aspect of Bookstein's (1991) approach to studies of form is that simple linear vectors (i.e., the distance between two landmarks) and angles cannot be considered to represent homologous characters (Bookstein, 1994). The true nature of the morphometric relationships among a set of objects can only be identified by simultaneous analysis of the entire set of landmarks. Further, because shape space is non-linear, this analysis is conducted in the context of a reference landmark configuration that defines the tangent space in which distances among objects may be treated as linear distances (Rohlf, 1996).

One technique developed by Bookstein (1991 and references therein) is the method of relative warps, derived by applying the thin-plate spline interpolating function to the landmark configurations of a set of objects. Perhaps the most lucid starting points for learning about relative warps are Rohlf (1993a, 1996). In essence, the interpolating function is derived for a reference landmark configuration (most often, the consensus configuration for the objects being studied) and then applied to each of the objects to determine its deviations from the reference configuration. These deviations, collectively for each object, are referred to as partial warp scores and may be thought of simply as a set of variables describing each object's location in the tangent space. Relationships among all objects can be examined by conducting a principal components analysis of the matrix of partial warp scores and projecting the objects onto the eigenvectors, which are now termed relative warps (Rohlf, 1996).

Deviations in the shape space (Kendall's shape space; Rohlf, 1996) consist of two components: affine and nonaffine transformations. Affine transformations are those applied uniformly (hence, the expression "uniform shape component") to the entire set of landmarks. In an affine transformation, all lines that are parallel before the transformation (e.g., a square) remain parallel following the transformation (the square transformed to a parallelogram by a shear). As Rohlf (1996) notes, "The effects of an affine transformation are of infinite scale since the effects of these changes cannot be localized to any particular region of an organism". Partial warps, on the other hand, "correspond to the nonaffine part of the thin-plate spline function that transforms the coordinates of the reference…into those of a particular specimen" and the partial warp scores (from which the relative warps are derived) "express the nonaffine shape differences between the reference and the ith specimen…" (Rohlf, 1996). Nonaffine transformations are those describing localized shape change within a landmark configuration. Although relative warps analysis was initially described with reference to just the partial warp scores (i.e., the uniform component was excluded; Rohlf, 1993a, 1996), Rohlf (pers. comm.) recommends that both components of shape be included in the analysis; two analyses, one with and the second without the uniform component, can reveal the relative importance of the uniform component.

Unfortunately, there appears to be a significant limitation to use of landmark methods with plant specimens: identifying biologically homologous landmarks that may be applied across an entire set of specimens. Jensen (1990) suggested that, within a group of leaf specimens, there are two landmarks that may be defined for all specimens: the juncture of blade and petiole (of course, this presumes the presence of a clearly defined petiole) and the apex of the leaf blade (assuming a well-defined midrib is present). This view appears applicable to a wide variety of dicotyledonous leaves, e.g., those of most woody species. However, to conduct an analysis of landmark configurations, one needs a minimum of three landmarks. Do additional landmarks exist on leaves? Jensen (1990), in an analysis comparing leaves of *Quercus palustris* Munchh. and *Q. velutina* Lam., identified additional landmarks based on the first three primary veins on each side of the leaf, employing both the origins and apices of these veins, and the bases of the leaf sinuses immediately above the lobes defined by the first and second veins. The last four, subjectively defined with reference to the midrib and the subtending lobe, represented what Bookstein & al. (1985) referred to as computed-homologies, i.e., they were "interpolated between appropriate landmarks" [Bookstein (1991) referred to landmarks such as these, i.e., "valleys of invaginations", as Type 2 homologies]. Jensen & al. (1993) and McLellan & Endler (1998) used similar criteria for identifying landmarks.

But, what does one do when some or all of the specimens at hand do not allow recognition of more than two biologically homologous landmarks? In many cases, closely related species have leaf architectures that differ dramatically: oaks have entire versus deeply lobed leaves and maples have simple versus compound leaves. Clearly, the set of landmarks identified for leaves of *Acer rubrum* L., which has simple, palmately veined, lobed leaves, cannot be applied to *A. carpinifolium* Siebold & Zucc., which has simple, pinnately veined, unlobed leaves. One approach to such situations has been to employ a suite of computed-homologies (Bookstein & al., 1985). For example, Dickinson & al. (1987) generated a set of "pseudolandmarks" (reflecting topographic homology) on the margins of hawthorn leaves based on the intersection of the long and short axes (length and width) of the leaf. Because there is no a priori reason to argue that the widest point of one leaf is biologically

homologous to that of another leaf, these landmarks cannot be assumed to represent true homologies. On the other hand, Paler & Barrington (1995) defined all of their landmarks based on supposed biological homologies. There was, however, another potential problem in both studies: Dickinson & al. (1987) did not indicate if leaf images were standardized for abaxial/adaxial orientation whereas Paler & Barrington (1995) ignored abaxial/adaxial orientation in favor of another criterion (the leaf apex must curve to the right). Failure to pay attention to abaxial/adaxial orientation may yield misleading results; a landmark identified at location x in abaxial view is not the same as a landmark identified at location x in adaxial view (except for the trivial cases where the landmark is located on a line connecting the base and apex of the leaf or where the leaf is perfectly symmetric about the central axis).

A potential shortcoming of landmark analyses is that little can be said of the features of the leaf that lie between the landmarks, especially when the landmarks are located on the margins of the leaves. Is the margin of the blade entire, dentate, serrate, or secondarily lobed? This information, which is a component of leaf shape, is not included in a landmark analysis. Thus, methods based on leaf outlines may be quite useful. This is the rationale for using such methods as calculating the fractal dimension, index of dissection, or deriving Fourier harmonics of the leaf outline [see McLellan & Endler (1998) for discussions of these methods]. In addition, Ray (1992) combined both landmark and outline data by using the landmarks to demarcate "homologous contours" on the outline followed by eigenshape analysis (Lohmann, 1983) of each contour. In his example, Ray (1992) found this approach superior to conducting a single eigenshape analysis of the entire outline. Ray's "landmark eigenshape analysis" does make use of landmark information, but it says nothing about the relative relationships among the landmarks themselves. While Ray's (1992) method apparently has not been used by any other researchers, there are (as noted above) numerous examples of the utility of outline methods for examining leaf shape variation.

The intent of this study was to compare three types of data in exploratory analyses of a sample of leaves: (1) a series of linear and angular measures, (2) coefficients derived from leaf outlines, and (3) partial warp scores derived from leaf landmark configurations. The leaves employed in this study represent two species of maple, *Acer rubrum* L. (red maple) and *A. saccharinum* L. (silver maple) and their hybrid (*A.* ×*freemanii* Murray). Red maple and silver maple occur commonly throughout eastern North America and both may be relatively abundant in swampy and mesic habitats, e.g., bottomlands, floodplains, and streambanks (Elias, 1980). Nevertheless, in our experience, while one or the other may be a dominant tree in such forests, it is unusual for both to be abundant in the same stand of trees. The two species are generally easily differentiated by leaf characters (especially such shape features as number and size of lobes and depth of sinuses) and there are conspicuous differences with respect to floral and fruit morphology as well.

A hybrid of these two species was created artificially in 1933 by Oliver Freeman, but naturally occurring hybrids were not reported until 1969 (Murray, 1969). Subsequently, naturally occurring hybrids have been reported from at least six states east of the Mississippi River (BONAP, 2001). These hybrids are characterized by intermediate leaf forms, although the range of leaf forms in Freeman's original crosses extends to leaves typical of both parental species (Hess & Crowley, 1990). The hybrids also exhibit intermediacy with respect to leaf trichomes, floral characters (including perianth structure and pubescence), and pollen morphology (Hess & Crowley, 1990). A number of cultivars of *A.* ×*freemanii* are distributed by nurserymen and these are often grown in arboreta. Access to hybrid trees of known provenance was an impetus for choosing these two species of maple for *exploratory* analyses of leaf shape differences.

Our working hypothesis was that leaf characters alone would allow us to differentiate the two species and that the hybrids would demonstrate morphological intermediacy. We expected this to be true for all three data types (linear and angular measures, outline descriptors, landmark configurations). Although Wilson (1992) concluded that multivariate methods, especially principal components analysis, are "used (incorrectly) to show hybridity", RJJ's experience is that multivariate methods are effective in allowing one to infer the presence of hybrids in a sample of OTUs [e.g., Knops & Jensen (1980) and Jensen (1988)].

MATERIALS AND METHODS

Leaf samples (vouchers have been deposited at ND; Table 1) were collected on 9 Jun 1998 from six trees of *A.* ×*freemanii* growing at the Morton Arboretum (Cook County, Illinois, U.S.A.). These trees consisted of three (**R99, S99, T100**) from one parental accession and three (**V98A, V98B, X98**) from a second parental accession (the identifiers in bold are the Morton Arboretum accession codes for these trees and these will appear in bold throughout the manuscript). Several branches with mature leaves, growing in sun-exposed portions of the lower crown, were harvested from each tree and all leaves were detached from the twigs and pressed by standard methods. On 22 Jun 1998, similar samples were

Table 1. Identities, locations, and collectors of the trees sampled. Voucher specimens are deposited at ND.

Taxon	Tree ID	Location	Collectors
Acer ×freemanii	**R99**	Illinois, Morton Arboretum, Cook Co.	*Jensen & Ciofani 1*
	S99	Illinois, Morton Arboretum, Cook Co.	*Jensen & Ciofani 2*
	T100	Illinois, Morton Arboretum, Cook Co.	*Jensen & Ciofani 3*
	V98A	Illinois, Morton Arboretum, Cook Co.	*Jensen & Ciofani 4*
	V98B	Illinois, Morton Arboretum, Cook Co.	*Jensen & Ciofani 5*
	X98	Illinois, Morton Arboretum, Cook Co.	*Jensen & Ciofani 6*
Acer rubrum	R19–R22	Indiana, St. Joseph Co.	*Jensen & Ciofani 11–14*
	R1–R18	Indiana, St. Joseph Co.	*Jensen & Miramontes 15–32*
Acer saccharinum	S1–S14	Indiana, St. Joseph Co.	*Jensen & Miramontes 1–14*
	S15–S18	Indiana, St. Joseph Co.	*Jensen & Ciofani 7–10*

taken from four trees each of red maple (R19–R22) and silver maple (S15–S18); for each species, two trees were growing naturally on land adjacent to the Saint Mary's College campus (St. Joseph County, Indiana, U.S.A.) and two trees were under cultivation on the campus. On 21 Jun 2000 and 26 Jun 2000, the same methods were used to collect leaf samples from 14 silver maples (S1–S14) and 18 red maples (R1–R18), respectively, from areas adjacent to the Saint Mary's College campus. The two areas from which naturally occurring trees were sampled were selected because, in RJJ's experience (18 years of transect sampling during an ecology course), each area appeared to represent a "pure population" of each species; i.e., no red maples had been observed in the area from which the silver maples were sampled and vice-versa. Thus, the trees were designated either red maple or silver maple as a function of location, *not* by reference to morphological characters.

The sets of leaves for each of the 46 trees (OTUs; operational taxonomic units) were carefully examined and only intact leaves, i.e., those with no visible damage along the margins, were selected for analysis, yielding sample sizes of 8–39 (mean = 23) leaves per tree. Petioles were carefully removed from all leaves to facilitate automatic capture of the leaf blade outlines. Individual leaves were placed on a lightbox, abaxial side up with the long axis (determined by blade base and apex) in a standardized orientation, and outlines were captured using MorphoSys (Meacham & Duncan, 1991). All outlines were initiated at the base of the leaf blade (landmark 1; Fig. 1) and were traced in a counterclockwise direction. Ten landmarks (Fig. 1) were designated for each leaf. These were defined by reference to the midrib (landmarks 1 and 6), the first (landmarks 4 and 8) and second (landmarks 2 and 10) veins to the right and left of landmark 6 that terminated at the leaf margin (i.e., corresponded to lobes), and bases of the sinuses immediately above these lobes (landmarks 5, 7 and 3, 9, respectively). We consider all of these to be Type I landmarks; however, the last four are supported as much by geometric as by histological evidence and may be considered Type II landmarks [see Slice & al. (1996) for landmark definitions].

The MorphoSys image files were used to create three

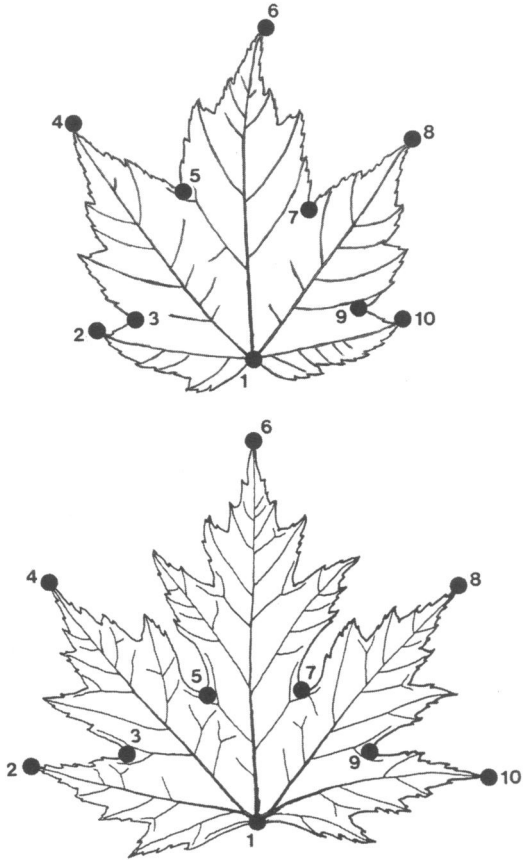

Fig. 1. Drawings of red maple (top) and silver maple (bottom) leaves illustrating locations of landmarks (see text for explanation; drawings modified from Voss [1972–1996]).

separate sets of data for analysis. First, a MorphoSys command file was written to generate a series of linear and angular characters (Fig. 2) as well as perimeter and area for each leaf. These files were converted to SYSTAT (ver. 6.0 for Windows) data files; mean vectors for 11 characters (Table 2) and mean leaf dissection (as defined by McLellan, 1993) were calculated for each tree and exported to NTSYSpc (version 2.1; Rohlf, 2000) compatible files. The 46 OTU × 11 character data matrix was standardized by characters (0 mean, unit variance) and used to create an OTU × OTU average taxonomic distance matrix as well as a character × character correlation matrix. A UPGMA (unweighted pair group method using arithmetic averages) phenogram and minimum spanning tree (MST) were constructed from the distance matrix. Principal components analysis (PCA) was performed on the correlation matrix and the OTUs were projected onto the resulting components. A second OTU × OTU distance matrix, derived solely from the measure of leaf dissection, was used for creating another UPGMA phenogram.

Second, the original MorphoSys chain codes for each leaf were converted to NTSYSpc compatible files of x, y coordinates using a program written by RJJ. These x, y files were used to generate the first 30 elliptic Fourier (EF) harmonics for each leaf. A program written by RJJ generated a file consisting of the mean EF harmonics for each OTU. The resulting 46 × 120 (four coefficients for each EF harmonic) matrix was used to create a 46 × 46 OTU distance matrix for UPGMA cluster analysis and a 120 × 120 variance-covariance matrix for PCA. As above, OTUs were projected onto the resulting components. In addition, a MST was created from the distance matrix and the IEF (inverse elliptic Fourier) option in NTSYSpc was used to create the mean leaf outline for each OTU.

Third, the landmark data from the original MorphoSys files were captured and converted to NTS file format by another program written by RJJ. TpsSmall (Rohlf, 1998) was used to determine how well the among-OTU Euclidean distances in the tangent space approximate the Procrustes distances in shape space [see Rohlf (1996) for a clear explanation of these two shape spaces]. TpsRelw (Rohlf, 1997) was used to create a consensus landmark configuration for each OTU. The 46 consensus configurations were then subjected to relative warps analysis, using the default settings in TpsRelw. The **W** (weight) matrix output by TpsRelw, including the

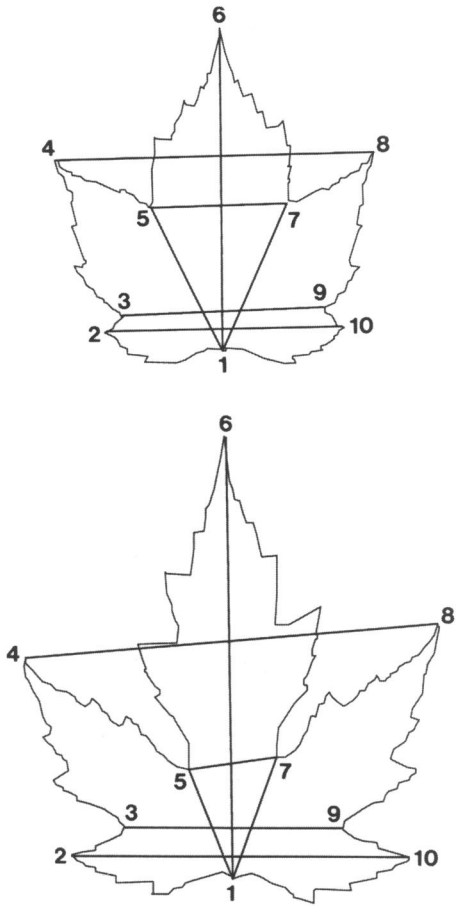

Fig. 2. MorphoSys chain code images of red maple (top) and silver maple (bottom) illustrating linear measurements described in Table 2. The four angles described in Table 2 are based on the following landmark triplets: 4-1-6, 8-1-6, 2-1-4, 10-1-8.

Table 2. Linear and angular characters and their loadings on principal components 1 and 2 from PCA of the character × character correlation matrix.

Character	PC1	PC2
Leaf length	0.317	0.770
Distance between upper lobe apices	-0.195	0.938
Distance between lower lobe apices	-0.054	0.688
Distance between upper lobe sinus bases	0.756	0.425
Distance between lower lobe sinus bases	0.634	0.726
Distance from blade base to left upper sinus base	0.923	0.298
Distance from blade base to right upper sinus base	0.918	0.314
Angle formed by left upper lobe, blade base, and apex	-0.784	0.436
Angle formed by right upper lobe, blade base, and apex	-0.795	0.388
Angle formed by left lower lobe, blade base, and left upper lobe	-0.744	0.499
Angle formed by right lower lobe, blade base, and right upper lobe	-0.793	0.439

uniform component, was modified for input to NTSYSpc for UPGMA cluster analysis (average taxonomic distances calculated directly from the **W** matrix), PCA (based on the variance-covariance matrix for the columns in the **W** matrix) and projection as described above. A second analysis, with the uniform component omitted, was performed to evaluate the relative contribution of the uniform component to the overall pattern of relationships among the OTUs.

Finally, patterns of among-OTU relationships in each of the four distance matrices were evaluated by Mantel tests (Mantel, 1967) of the hypothesis that the elements of two symmetric distance matrices are independent of one another. If the hypothesis is rejected, then we may assume that the patterns of among-OTU relationships are concordant in the two matrices, i.e., OTUs that have low (or high) dissimilarity in one matrix will illustrate low (or high) dissimilarity in the second matrix. The six matrix comparisons were performed using the MXCOMP procedure, with 1000 permutations, in NTSYSpc.

RESULTS

As shown in Figure 3, a traditional morphometric analysis based solely on simple linear and angular measures yields several well-defined clusters. There are two obvious outliers (R21 and S13), one of each species, but most individuals field identified as either red or silver maple are found within the same general clusters: a silver maple cluster (reading from top to bottom in Fig. 3, OTUs S1–S12) and a red maple cluster (OTUs R1–R16). In addition to the two outliers, two other OTUs appear "misplaced": red maples R4 and R18 cluster with the silver maples. Four hybrid OTUs (**S99, V98A, V98B, X98**) are found in a single well-defined cluster within the larger red maple cluster while the other two (**R99, T100**) are in the silver maple cluster. The cophenetic correlation (r_{CS}) for this phenogram, 0.761, indicates a "fair" (Rohlf, 1993b) fit between the OTU × OTU distances implied by the phenogram and the actual among-OTU distances.

These relationships can also be seen in Fig. 4, a projection of the OTUs onto the two-dimensional space defined by the first two principal components. The first component, accounting for 47.6% of the total variation, separates most of the silver and red maples, but there is no clear break between the two known "groups". The connection between the two groups (as shown by the MST) is through OTUs R19 and S11. However, as in Fig. 3, red maples R4 and R18 group with the silver maples. In addition, silver maples S7 and S17, despite being near the silver maple group in this two-dimensional space and

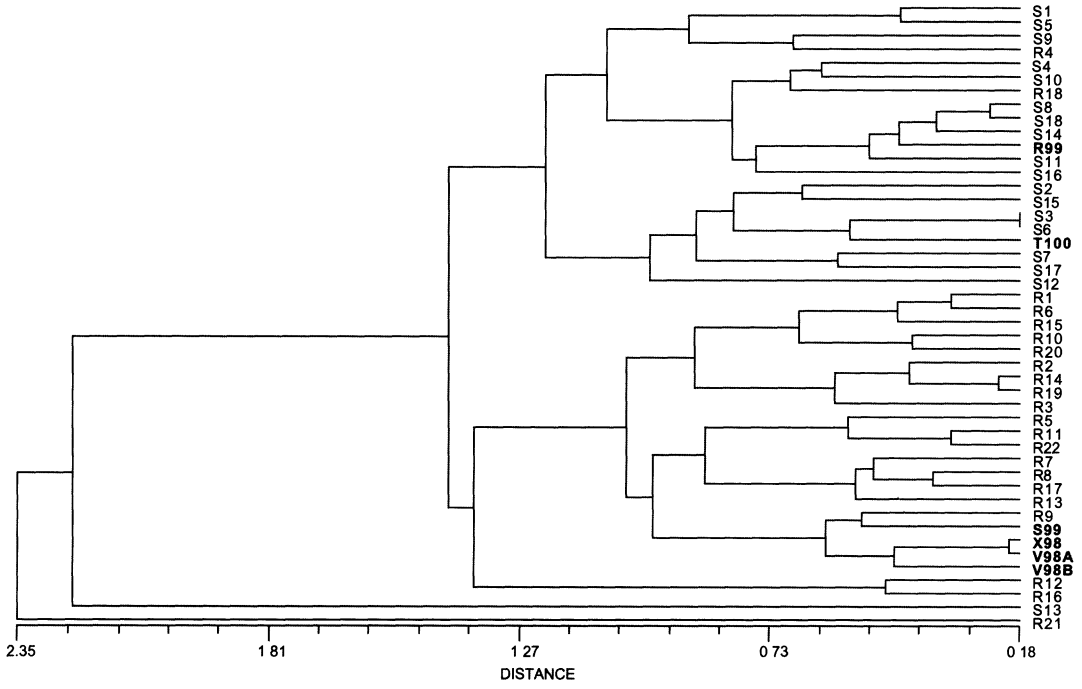

Fig. 3. A UPGMA phenogram derived from a matrix of average taxonomic distances based on 11 linear/angular characters (Table 2). r_{CS} = 0.761. R1-R22 are OTUs tentatively identified as red maples; S1-S18 are OTUs tentatively identified as silver maples; R99, S99, T100, V98A, V98B, and X98 are OTUs of known hybrid parentage (see text for additional details).

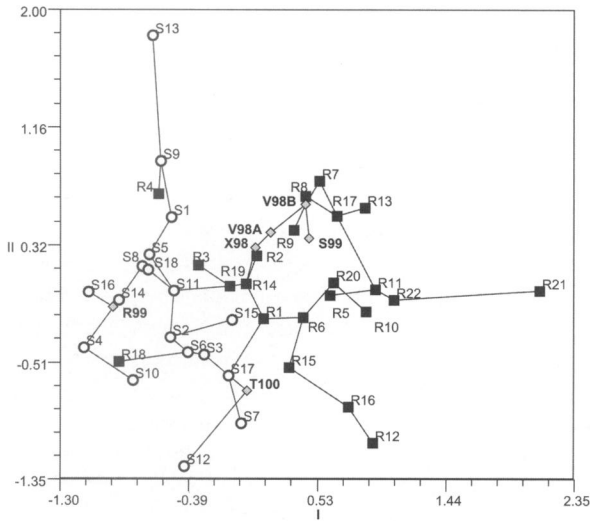

Fig. 4. OTUs projected onto the first and second components of a PCA based on a matrix of character x character correlations. A minimum spanning tree derived from the full OTU x OTU distance matrix is superimposed. Black boxes = red maples, open circles = silver maples, gray diamonds = hybrids. OTU labels as in Fig. 3. Percent variance explained: component 1 = 47.6 %, component 2 = 33.0 %. rCS = 0.965.

clustering with silver maples in Fig. 3, have their MST connection (based on the full dimensional space) to the red maple group. As in Fig. 3, four hybrids group with red maples and two with silver maples. Hybrid **T100** is, in this two-dimensional space, positioned well toward the red maple side of component one (along with silver maples S7 and S17). The among-OTU distances in this reduced two-dimensional space are a "very good" fit to the overall among-OTU distances (r_{CS} = 0.965).

As seen in Table 2, the first component has very high loadings for the two sinus depth characters and moderately high loadings for the two between-sinus-base lengths as well as for all four angles. The second component, accounting for 33.0 % of the total variation, emphasizes variation within the two groups (Fig. 4). One character, distance between upper lobe apices, dominates the second component while three others (blade length, distance between lower lobe sinus bases, distance between lower lobe apices) have moderately high loadings. If we ignore the two outliers (R21, S13), then both species illustrate similar degrees of variation in this two-dimensional space.

The single-parameter descriptor, leaf blade dissection, yields a phenogram (Fig. 5) with three well-defined clusters. As in Fig. 3, there are two outliers (cluster S5 + R18), one of each species (but they are not the same outliers as in Fig. 3), and there are two clusters (reading top to bottom, OTUs S1–S17 and OTUs S7–R21) that correspond to the two species. Again, two red maples (R4, R9) cluster with the silver maples. However, one silver maple

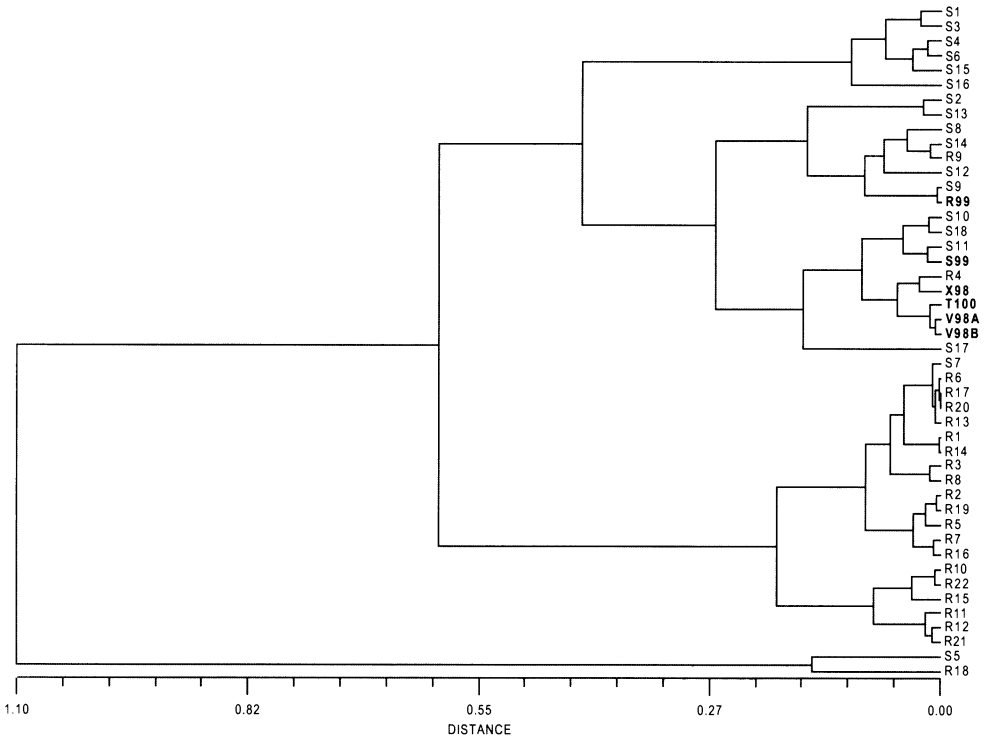

Fig. 5. A UPGMA phenogram derived from a matrix of average taxonomic distances based on the single-parameter character, leaf dissection. r_{CS} = 0.803. OTU labels as in Fig. 3.

(S7) now clusters with the red maples and all of the hybrids are found in the silver maple cluster. Despite the compact structure of the phenogram, r_{CS} is only 0.803, barely qualifying as a "good" fit (Rohlf, 1993b) between the implied and actual distances.

A more detailed analysis of the leaf outlines, using EF harmonics, provides a different view of relationships (Fig. 6) than found with the single-parameter analysis (Fig. 5). First, the clusters are not as compact. Second, there appear to be five general clusters: S1–R9, R1–R4, S2–S13, S7–R21, and R18–S16 (reading top-to-bottom in Fig. 6). The second of these clusters consists exclusively of red maples with three of the hybrids while the first and third consist primarily of silver maples, the former including two hybrids and one red maple and the latter including one hybrid and one red maple. The last two of the five clusters each consists of three OTUs, two of one species and one of the other. The images adjacent to the OTU labels in Fig. 6, the average leaf outlines reconstructed from the mean EF coefficients, provide some insights into the aspects of shape that each cluster emphasizes. For example, the two silver maple clusters differ with respect to the width of the blade bases and the three outliers (R18, S15, S16) appear to have deeper sinuses and narrower upper lobes than do the silver maples in the uppermost cluster. This phenogram yields a borderline "fair to good" fit (r_{CS} = 0.792) between implied and actual distances.

An alternative view of relationships derived from EF coefficients is presented in Fig. 7, a plot of OTUs in the two-dimensional space defined by the first two principal components from the among-coefficients variance-covariance matrix. The first two components account for 71.6 % (45.2 % and 26.4 %, respectively) of the total variation. Neither component emphasizes between-species differences: the two species are separated primarily along the upper left–lower right diagonal. Four red maples (R5, R7, R9, R18) fall on the silver maple side of the diagonal and one silver maple (S7) falls on the red maple side. The MST connections support the cohesiveness of these two groups and for this ordination, despite some rather long MST connections, r_{CS} = 0.964, a "very good" fit. Four of the hybrids (**S99, V98A, V98B, X98**) fall very close to the diagonal and a fifth (**T100**) is linked to them by MST connection. The last hybrid, R99, is located in the midst of the silver maple group.

Despite rather obvious differences in leaf shapes (e.g., Figs. 1, 6), there is little distortion of Procrustes

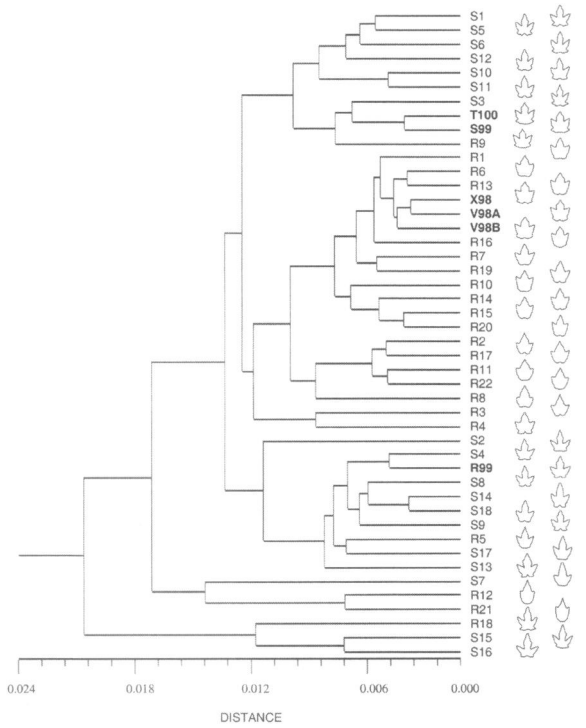

Fig. 6. A UPGMA phenogram derived from a matrix of average taxonomic distances based on the coefficients for the first 30 elliptic Fourier harmonics of the leaf outlines. r_{CS} = 0.792. OTU labels as in Fig. 3. Images to the right of each label are the average leaf outlines for that OTU.

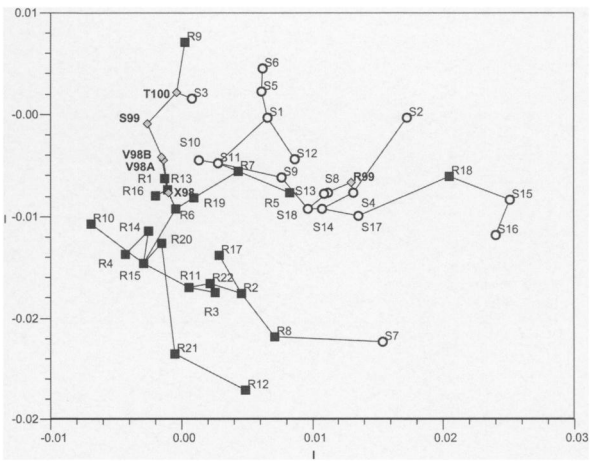

Fig. 7. OTUs projected onto the first and second components of a PCA based on a matrix of character x character covariances (characters are EF coefficients; see text). A minimum spanning tree derived from the full OTU x OTU distance matrix is superimposed. Black boxes = red maples, open circles = silver maples, gray diamonds = hybrids. OTU labels as in Fig. 3. Percent variance explained: component 1 = 45.2 %, component 2 = 26.4 %. r_{CS} = 0.964.

distances when the OTUs are projected onto the tangent plane (r = 0.999977). Cluster analysis of distances derived from the full **W** matrix yields the phenogram in Fig. 8: there are two primary clusters (S1–S11, S7–R21) and one outlier (R8). The two clusters represent silver maples and red maples, respectively, but there are some "misplaced" OTUs: one red maple (R18) clusters with the silver maples and two silver maples (S7, S17) cluster with the red maples. The six hybrids also cluster with the red maples. The cophenetic correlation for this phenogram (r_{CS} = 0.803) is at the low end of the "good" (Rohlf, 1993b) category.

The PCA ordination (Fig. 9; the components are identical to the relative warps generated by TpsRelw) shows clear separation of the two species groups (the two clusters noted in Fig. 8) along the first relative warp, with five of the hybrids occupying positions intermediate to the two species (hybrid **R99** again is well within the silver maple group). The cohesiveness of the two groups is revealed by the MST connections, and the path connecting the two groups passes through the group of hybrids in the upper center of Fig. 9. These two relative warps account for 72.5 % (43.7 % and 28.8 %, respectively) of the variation in the weight matrix and this two-dimensional view is a "very good" (Rohlf, 1993b) representation (r_{CS} = 0.927) of the actual among-OTU distances derived from the weight matrix.

When the uniform component is omitted, the results (not shown) are essentially identical to those for the full **W** matrix. The two phenograms are topologically identical and the two-dimensional ordination with the MST superimposed cannot be differentiated from that shown in Fig. 9. In fact, deleting the two columns representing the uniform component has no effect, to eight decimal places, on any of the eigenvalues. Because the uniform component represents two additional characters, there are minor increases in the percent variance accounted for by each relative warp; warp one increases from 44.804 % to 44.817 % and warp two increases from 28.936 % to 28.945 %. Further, r_{CS} between a distance matrix based solely on the nonaffine shape components and a distance matrix based solely on the uniform component is only 0.061; i.e., relationships among OTUs on the uniform component are unrelated to those based on the nonaffine components. A plot of OTUs in the two-dimensional space defined by the x and y uniform components (not shown) reveals no pattern corresponding to the taxonomic origin of the OTUs. Thus, the uniform component con-

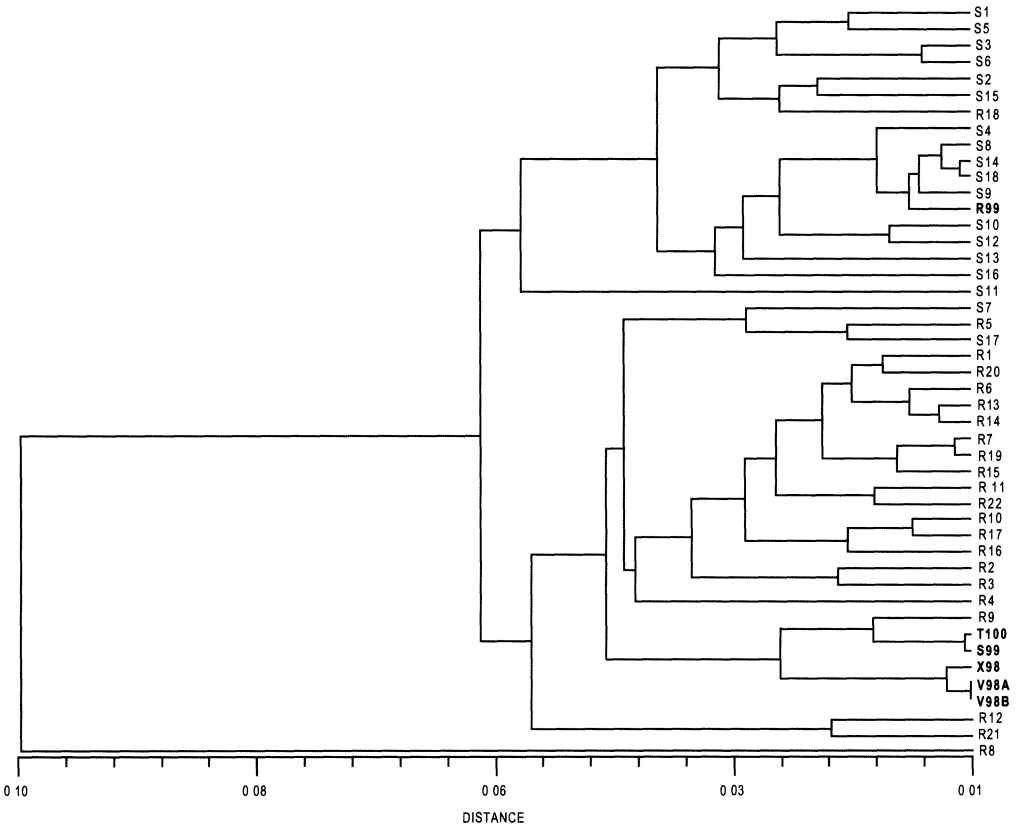

Fig. 8. A UPGMA phenogram derived from a matrix of average taxonomic distances based on the W matrix from a relative warps analysis (see text for explanation). r_{CS} = 0.803. OTU labels as in Fig. 3.

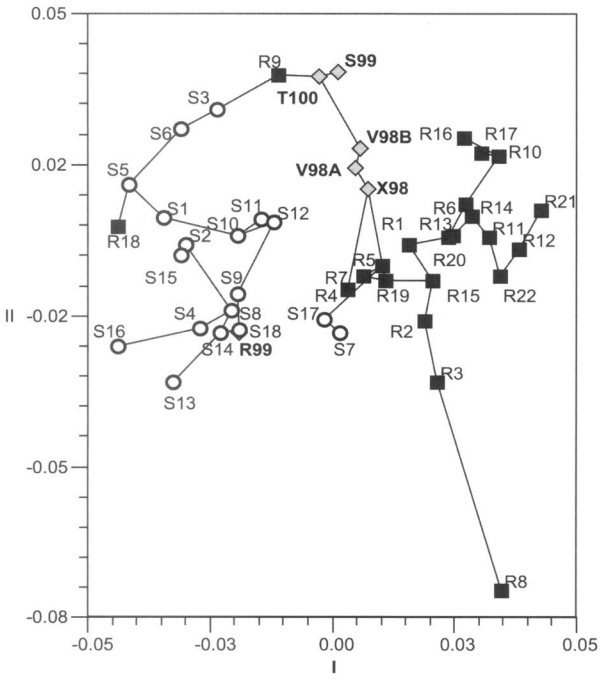

Fig. 9. OTUs projected onto the first and second components of a PCA based on a matrix of character x character covariances (characters are elements of the W matrix from a relative warps analysis; see text for explanation). A minimum spanning tree derived from the full OTU x OTU distance matrix is superimposed. Black boxes = red maples, open circles = silver maples, gray diamonds = hybrids. OTU labels as in Fig. 3. Percent variance explained: component 1 = 44.8 %, component 2 = 28.9 %. r_{CS} = 0.927.

tributes little to our understanding of among-OTU relationships.

Finally, despite differences in the methods, all provide similar views of relationships among these 46 OTUs. Mantel test statistics (Table 3) range from a low of 0.413 (comparing distances based on linear/angular characters with those based on EF coefficients) to a high of 0.639 (comparing distances based on EF coefficients to those based on relative warps weights). Despite the wide range, all of the values in Table 3 are highly significant ($p <= 0.001$).

Table 3. Mantel tests of the relationships among three distance matrices. The values presented are the normalized Mantel test statistic (Z). For all tests, the one-tailed probability that a randomly generated value of Z ≥ the observed value of Z is 0.001.

	Leaf dissection	Elliptic Fourier coefficients	Relative warps weights
Linear/angular characters	0.513	0.413	0.496
Leaf dissection		0.521	0.555
Elliptic Fourier coefficients			0.639

DISCUSSION

One thing that is clear, and not necessarily surprising, is that each of these analyses, including that based on a single variable, allows recognition of two core groups corresponding to the two species. These core groups can be seen in each ordination (Figs. 4, 7, 9) but appear in only three of the four phenograms (Figs. 3, 5, and 8). The fourth phenogram, derived from EF coefficients (Fig. 6), breaks the silver maples into two distinct clusters, one of which joins with the red maple cluster rather than the other silver maple cluster.

A second point is that each analysis depicts one or more OTUs as outliers with respect to the core groups. In Fig. 3, red maple R21 and silver maple S13 appear as two separate single-OTU clusters and there is no indication of their actual affinities with other OTUs. The ordination for the same data (Fig. 4) reveals that these two OTUs are outliers on the first and second components, respectively. The reasons these two are outliers are easy to determine: among all OTUs, R21 has the shallowest upper sinuses and smallest lobe angles (for all four angles), while S13 has the longest leaf, greatest distance between upper lobe apices, and third greatest distance between lower lobe apices. As shown in Table 2, these are exactly the characters that have the highest loadings on components one and two, respectively.

In a sense, this is one of the strengths of traditional morphometrics: there are many instances in which the patterns seen can be tied rather clearly to one or a few of the measured characters. And, as is often the case, PCA may provide insights into shape and size differences. In Fig. 4, the second component appears to be a general size component (the highest loadings are for lengths and widths; Table 2) and the first component appears to be a general shape component (the highest loadings are for upper sinus depths and the four lobe angles; Table 2). The fact that "size" appears to be emphasized along component two is not what is usually expected; as noted by Bookstein & al. (1985; see additional references therein), general size variation is most often summarized by the first component. However, because each component is a linear combination of all characters, "size" and "shape" cannot be completely uncoupled [see Bookstein (1989) for an excellent discussion of the difficulties inherent in attempting to separate size and shape via traditional morphometrics].

There are also two outliers in Fig. 5. As with the previous case, it is relatively easy to determine why these two are outliers: OTUs S5 and R18 have dissection index values of 3.04 and 3.20, respectively. The next highest value is 2.70, for OTU S16. The pattern in Fig. 5, three primary clusters, is easy to decipher: the dissection index values for the small cluster (S5 + R18) average 3.12; the values for the silver maple cluster (S1–S17) range from 1.92 to 2.70 with a mean of 2.29; and the values for the red maple cluster (S7–R21) range from 1.51 to 1.84 with a mean of 1.70. Given that there is no overlap in the ranges for the three clusters, it is obvious that these means are statistically significantly different. The mean leaf outlines shown in Fig. 6 demonstrate the differences among these clusters. Although it is not clear why the outlines for OTUs S5 and R18 have the highest dissection values (S5 appears to be only subtly different from S1), the differences between "typical" silver maple outlines (e.g., OTUs S1 and S2) and "typical" red maple outlines (e.g., OTUs R1 and R14) are rather obvious.

Outlines are also the source for the data used to produce Figs. 6 and 7 (via EF analysis). In this case, however, the two species groups are not as cohesive (Fig. 6) as in the single-parameter analysis (Fig. 5). Most silver maples are in one of two distinct clusters and there are two reasonably well-defined clusters of outliers. One cluster of outliers consists of three OTUs (S7, R12, R21) with conspicuously rounded blade bases, greatly reduced lower lobes, and a central segment that is more narrowly triangular than in the other red maples. These three OTUs are typical of what has been recognized by some as *A. rubrum* var. *trilobum* K. Koch. On the other hand, the three OTUs (R18, S16, S17) in the other cluster of outliers, while appearing to have deeper upper sinuses than the silver maples in the top cluster (S1–R9), do not appear noticeably different from OTUs in the other cluster of silver maples (S2-S13).

The patterns seen in Fig. 6 are also seen in Fig. 7. In the two-dimensional ordination space, the silver maple OTUs are widely distributed along the first component, those near the upper center of the plot corresponding to the top cluster of silver maples (those that cluster with the core group of red maples) in Fig. 6. Unfortunately, there is no way for us to identify specific features of the leaves that are responsible for the pattern seen in Fig. 7. Examination of the loadings of the EF coefficients on the two components allows us to state that the four highest loadings on component one are (in decreasing order) for coefficients C3, C2, B2, and B4 [coefficients identified as in Rohlf (1993b)] and the three highest loadings on component two are for coefficients C1, C4, and B5. These quantities, individual sines or cosines for given harmonics, cannot be translated into morphological characters.

It may be possible to associate the principal components derived from EF coefficients with specific morphological characters. For example, Jensen & al. (in press) found, via regression analysis, that OTU scores on the first principal component were excellent predictors of the length/width ratio for the leaves examined (the correlation between the first component score and the ratio was -0.984). Using the same approach here, we find that the morphological variables (Table 2) having the highest correlations with component one in Fig. 7 are the distances from the blade base to the right and left upper sinus bases; however, these are only moderately strong (~-0.65) correlations. Similarly, two characters, distance between lower lobe apices and distance between upper lobe sinus bases, are moderately correlated (~0.59) with the second component in Fig. 7. Interestingly, the index of leaf dissection is moderately positively correlated (~0.61) with both components one and two. This should probably be expected in that both of the PCA components and the index of dissection are functions of the leaf outline.

Can we improve on these results? In our view, the answer is yes. In each of the first three analyses, information is lost (e.g., when using lengths and widths, the relative locations of the landmarks on which the measurements are based are ignored), it is possible for objects with quite different shapes to yield identical values (e.g., a leaf blade that is perfectly square and has the petiole attached at the midpoint of one of the sides has the same dissection value as a leaf blade that is a square with the petiole attached at one of the vertices; clearly, using the junction of blade and petiole as a reference, these leaf blades have different shapes), or the "characters" used for the analysis (EF coefficients) have no intrinsic morphological meaning. What is needed is an approach that uses all of the information contained in the original data, provides a unique set of descriptors for each shape (i.e., two different shapes cannot be the same distance from a reference shape), and yields results that are biologically interpretable. The method of relative warps analysis, based on the thin-plate spline interpolating function, does just that (Bookstein, 1996).

Cluster analysis (Fig. 8) based on partial warp scores [the **W** matrix of Rohlf (1993a, 1996)] resulted in two well-defined clusters, corresponding to the two species groups, and one conspicuous outlier (R8). Similarly, projection of the OTUs onto the first two relative warps (Fig. 9) reveals the same two groups, separated along the first relative warp, with OTU R8 well separated from all other OTUs along the second relative warp. The MST in Fig. 9 reflects the relationships seen in Fig. 8. In Fig. 9, the two major clusters are connected by MST links through the group of hybrids and between OTU **X98** and OTUs R4 and R19. Interestingly, the two primary clus-

ters (Fig. 3) derived from the set of eleven "traditional" morphological variables (Table 2) are perfectly defined by the set of MST connections in Fig. 4, and r_{CS} values for both Figs. 4 and 7 are higher than for Fig. 9. Doesn't this suggest that these other approaches are, in some sense, better?

To answer this question, we need to take a more careful look at the information provided by each analysis. As a beginning, Fig. 10 provides illustrations of relative warp deformations for selected OTUs as well as the consensus configuration with which these were compared. These OTUs were selected because they span the "shape space" illustrated in Fig. 9 and/or because they represent outliers in various analyses. For example, OTUs R21 and S13 are the outliers seen in Figs. 3 and 4. In Fig. 9, these two are located very close to OTUs R12 and S16, respectively. Examination of the relative warp deformations in Fig. 10 indicates that the landmark configurations for each pair (R12–R21, S13–S16) are quite similar. The primary differences between landmark configurations for S13 and S16 are that, relative to landmark 1, in the latter landmarks 5 and 7 are located closer to landmarks 4, 6, and 8 while landmarks 2 and 10 are closer to each other. These changes can be seen as an expansion of the grid between landmarks (5, 7) and (3, 9) with a simultaneous reduction in the curvature of the grid in the vicinity of landmarks 2 and 10. The differences between OTUs R12 and R21 involve an "inflation" of the grid that increases the distances among landmarks 3, 5, 7 and 9. Why, if these two pairs of OTUs have such similar landmark configurations, do they appear as outliers in Figs. 3 and 4? The answer is quite simple: in both cases there are marked differences in size. The seven linear measures (Table 2) for R21 are, on average, 45% greater than those of R12 and the same measures for S13 average 63% greater than those for S16. Both components in Fig. 4 have their highest loadings with two or more of these linear measures. Because all OTU landmark configurations are scaled to unit centroid size (Rohlf, 1996), isometric size differences effectively play no role in calculating among-OTU dissimilarities.

There are also two outliers in Fig. 5, based on the single-parameter measure of leaf dissection. In Figs. 3, 4, 8 and 9, these OTUs (R18, S5) are found in the silver maple clusters. However, in Figs. 6 and 7 (derived from EF coefficients), these two are in distinct clusters. Despite the similarity of their leaf dissection values and landmark configurations (Fig. 10), there are differences in their EF coefficients. The latter are more sensitive to changes in leaf outline than is leaf dissection. Low-order EF harmonics emphasize gross shape differences whereas higher-order harmonics reflect differences on a smaller scale (McLellan & Endler, 1998). This would explain why two OTUs with leaves having noticeably different outlines cluster together in Fig. 5, but are found in different clusters in Fig. 6 (e.g., OTUs S10-S18 and R3-R8). In this regard, both McLellan & Endler (1998) and Rumpunen & Bartish (2002), found that analyses of EF outline descriptors provided better discrimination among groups of OTUs than did linear measurements. McLellan & Endler achieved slightly better discrimination of a priori groups with a power series function of the EF coefficients than with the normalized EF coefficients; Rumpunen & Bartish (2002) reported just the opposite (Rumpunen & Bartish, however, found that the power series function yielded better results in cluster analysis).

Perhaps the best example of the way these methods differ with respect to a single OTU is the outlier (R8) seen in Figs. 8 and 9. As shown in Fig. 10, this OTU has a distinctive landmark configuration: landmarks 5 and 7 are relatively close to landmarks 4 and 8 (as in other red maples, e.g., R12 and R21 in Fig. 10), landmark 1 is closer to landmark 6, as in most silver maples (e.g., S13 and S16 in Fig. 10), and landmarks (2, 3) and (9, 10) are quite close together, again as in other red maples. In addition, there is a pronounced asymmetry at the base of the leaf blade. Inspection of the other deformation grids in Fig. 10 reveals that all landmark configurations are roughly symmetric with respect to a line connecting landmarks 1 and 6. [Symmetry is not to be ignored when using thin-plate spline methods. Bookstein (1996) notes that for a variety of multivariate procedures, perfect symmetry creates a serious problem—the covariance matrix is singular; however, he also notes that relative warps analysis "needs no modifications for symmetric forms". While geometric morphometrics can be used for studies of asymmetry (e.g., Klingenberg & McIntyre, 1998), that is not the focus of this contribution.] The consensus configuration in Fig. 10 reveals that most of these leaves are somewhat asymmetric: with respect to landmark 1, all other landmarks are rotated in a clockwise direction. If the leaves were perfectly symmetric, landmark pairs (4, 8), (5, 7), (3, 9), and (2, 10) would be expected to occupy identical positions, in an x, y basis, on opposite sides of the line connecting landmarks 1 and 6. Subtle asymmetries are seen in each of the deformation grids in Fig. 10. For example, in both R12 and R21, the distance between landmarks 9 and 10 is less than the distance between landmarks 2 and 3. Similarly, in both S13 and S16, the distance between landmarks 7 and 9 is less than that between 5 and 3.

What is interesting in this context is that the distinctive landmark configuration and marked asymmetry of OTU R8 apparently provide a very weak signal when linear measures or outlines are analyzed. In the other three analyses (Figs. 3-7), there is nothing to suggest that R8 is different from the other red maples. Clearly, the landmark configuration provides insights into shape that are

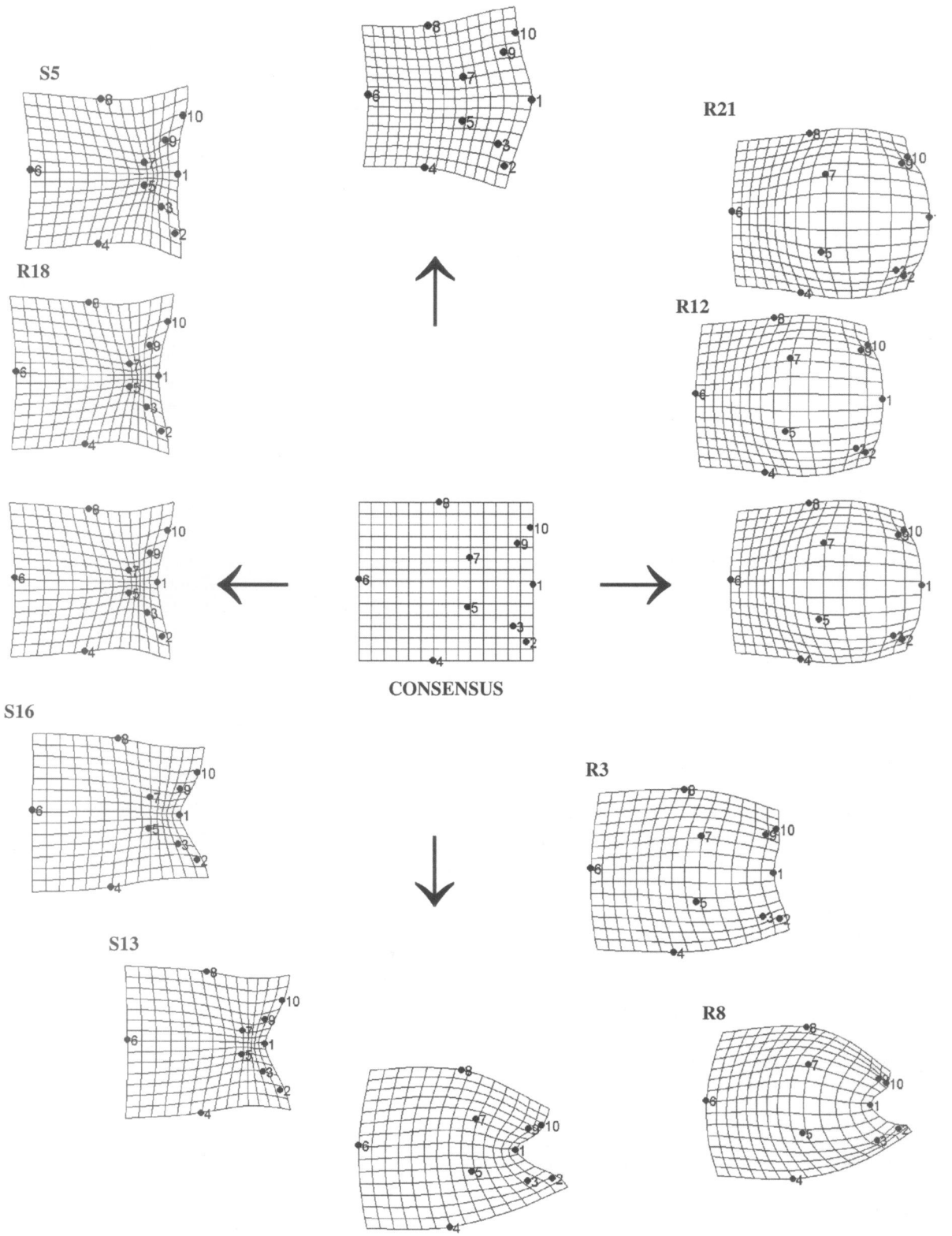

Fig. 10. Relative warp deformation grids for the first and second relative warps and selected OTUs. Center grid is the consensus landmark configuration; horizontal arrows point to positive (right) and negative (left) extremes of warp one; vertical arrows point to positive (top) and negative (bottom) extremes of warp two. OTU labels and relative positions as in Figure 9. Grids oriented with leaf base on the right, leaf apex on the left (compare with Fig. 1).

Table 4. Core groups that are found in all analyses and OTUs that are either outliers or "misplaced" in at least one analysis.

Core red maples	Misplaced or outliers	Core silver maples
R1		S1
R2		S2
R3		S3
	R4	S4
	R5, S5	
R6		S6
R7	S7	
	R8	S8
	R9	S9
R10		S10
R11		S11
	R12	S12
R13	S13	
R14		S14
R15	S15	
R16	S16	
R17	S17	
	R18	S18
R19		
R20		
	R21	
R22		

not detectable by traditional analyses or by outline analyses as conducted here. If our goal is to address differences with respect to shape, then we must use a method that is capable of detecting these differences. The advantage of geometric morphometrics is that it provides a single, complete, and biologically interpretable view of the information contained in the landmark configurations. The landmark configurations (Fig. 10) can be translated into some of the traditional characters used to differentiate these two species: silver maples (e.g., S13 and S16 in Fig. 10) have a narrower base for the central leaf segment (the distance between landmarks 5 and 7) and have much deeper upper sinuses (the positions of landmarks 5 and 7 relative to landmarks 1, 4, and 8) than do red maples. Both of these could be converted to key characters: for the former, if the width of the base of the central segment (line 5–7) is less than one-third the distance between the upper lobe apices (line 4-8), then the specimen is a silver maple; for the latter, if the line from blade base to upper sinus base (1-7) is less than one-half the length of the line from blade base to upper lobe apex (1–8), again, the specimen is a silver maple. Many keys to *Acer* species [e.g., those in Gleason (1968), Fernald (1970) and Voss [1972–1996)] make direct or indirect reference to both of these characters, although typically in more subjective terms.

One other interesting observation arises with respect to the relative warps analyses. For our samples, the uniform component of shape change has no appreciable effect on among-OTU relationships. The uniform component has been reported to be an important aspect of shape variation in several studies. For example, Carpenter (1996) reported that the uniform shape component summarized the primary differences among species of emperor fishes, and Bogdanowicz & Owen (1996) found that the uniform component was significantly different among species of plecotine bats and was correlated with size differences among their OTUs. On the other hand, Rohlf & al. (1996), in a study of Old World moles, and Monteiro (1999), in a comparison of tegu lizard skulls, both reported that the uniform component played a minor role in explaining shape variation. The low matrix correlation between the uniform and nonaffine matrices we report ($r = 0.061$), combined with the fact that, for all of our leaves, there is effectively no relationship between centroid size and the two uniform components ($r = 0.001$ and 0.034 for uniform x and uniform y, respectively, with centroid size) leads us to conclude, as did Rohlf & al. (1996), that "The uniform component does not seem to make an important contribution...for these data".

What about the relationships among the two species and their hybrids? The first general observation is that, despite which approach we use, there are two core groups (Table 4): 15 red maples consistently cluster together and 12 silver maples consistently cluster together. There are (Table 4) seven red maples and six silver maples that, in at least one of these analyses, either cluster with the other species or can be identified as outliers of uncertain affinity with respect to the two core groups. Two of these, OTUs S7 and S17, may be red maples growing in the area we identified as a silver maple area (see Methods). Both their leaf outlines and their landmark configurations suggest that they are red maples (Figs. 6, 8, 9). Similarly, R9 and R18 are usually found in the midst of the silver maple core group or as an outlier and may be silver maples growing in our red maple area.

On the other hand, we cannot discount the possibility that these misplaced and outlier OTUs may be of hybrid origin. In each ordination (Figs. 4, 7, and 9), five of the hybrid OTUs from the Morton Arboretum appear intermediate between the two core groups. The sixth hybrid (**R99**), in every analysis, is firmly ensconced in the midst of the silver maple core group. Hybrid **R99** is derived from the same parental accession as hybrids **S99** and **T100**, yet these three do not consistently cluster together (although **S99** and **T100** do cluster together in

Figs. 6–9). Conversely, the other three hybrids appear in a discrete cluster in every analysis (joined by **T100** and R4 in Fig. 5). As noted by Hess & Crowley (1990), F_1 plants from Freeman's original crosses exhibited leaf morphologies that ran the gamut from typical red maple to typical silver maple. Thus, it might not be surprising that trees of hybrid origin would cluster with one or the other of the parent species (as does OTU **R99**). However, what is surprising is that trees from the same parental accession would show such wide variation. Hybrids **R99**, **S99** and **T100** are derived from a single parental tree, as are hybrids **X98**, **V98A**, and **V98B**. While the last three are morphologically similar by all measures we have employed, the former three exhibit a pronounced difference in leaf morphology. Comparisons of the mean leaf outlines in Fig. 6 reveal that, at that scale, the outlines of **X98**, **V98A**, and **V98B** are almost identical. While the same may be said for **S99** and **T100**, the outline for **R99** can be differentiated from those of its siblings. The morphological differences are much more apparent in Fig. 11. The deformation grids for the first set of hybrids (**X98**, **V98A**, **V98B**) are essentially identical (there are subtle differences in the relationships among landmarks 1, 2, 3, 9, and 10), as are the deformation grids for hybrids **S99** and **T100** (in **T100**, all landmarks except 6 are slightly closer to landmark 1 than for **S99**). The deformation grid for **R99**, however, is noticeably different from the other five: the base of the leaf is narrower (landmark pairs 2–3 and 9–10 are closer together) and concave (landmark 1 is much closer to landmark 6). These differences explain why **R99** clusters with silver maples rather than with its siblings or red maples (Figs. 8 and 9).

Why is **R99** so different from the other five hybrids? There are at least three plausible explanations. First, the stock for **R99** may have been mislabeled prior to accession by the Morton Arboretum or, failing that, prior to being planted at the Arboretum. Second, **R99** and its two siblings may have been reproduced by seed, rather than by cuttings. If so, then the differences in **R99** could be the result of genetic segregation. Third, if **R99** was taken as a cutting from the same stock as **S99** and **T100**, then we could hypothesize a somatic mutation that led to the quite different leaf shape. Because we have been reassured that no mislabeling occurred and that **R99**, **S99**, and **T100** were derived from wild seed collected from a parent tree of putative hybrid origin (W. H. Hess, pers. comm.), it seems reasonable to assume that the differences among these three reflect genetic segregation in the F2 generation. The other three hybrids (**X98**, **V98A**, **V98B**) were derived as grafts from a single tree, hence their high degree of similarity.

There is another interesting point with respect to the morphologies of the hybrids. *Acer* ×*freemanii* is described by Gelderen & al. (1994) as having leaves that "though smaller than those of *A. saccharinum* are more deeply dissected, [and] have the same general shape". Our samples do not fit this description. They are equally as large as silver maple leaves and there is nothing to suggest that they are more dissected. Further, with respect to shape, as defined by EF coefficients (Fig. 7) or landmark configurations (Fig. 9), they appear (with the exception of **R99**) to be morphologically intermediate between the two species. While Wilson (1992) has shown, through simulations, that multivariate approaches cannot be expected to allow one to infer hybridity, we believe these results provide yet another in a long list of examples in which hybridity can be inferred from a multivariate analysis. It seems likely that several of our naturally occurring OTUs, e.g., R18 and S17, represent hybrids that were not detected prior to the analyses.

Finally, any one of these analyses could be considered an appropriate means for examining morphological relationships among these two taxa and their hybrids. The highly significant Mantel test statistics (Table 3) indicate general agreement among the overall patterns of among-OTU relationships. Additionally, all analyses separated **R99** from the other hybrids and led to recognition of OTUs that were either misidentified (e.g., S7) or may represent naturally occurring hybrids (e.g., S17 and R18). However, only the thin-plate spline approach was sensitive to the differences between R8 and the other red maples. While traditional morphometrics and outline methods clearly have their place (when landmark methods are not applicable), we believe that geometric morphometrics should be used whenever the specimens under study allow recognition of an appropriate suite of landmarks.

ACKNOWLEDGEMENTS

This contribution is dedicated to F. James Rohlf on the occasion of his recent retirement. A friend and mentor to RJJ for the past 26 years, Jim authored most of the software used in our analyses and provided valuable comments on an earlier version of the manuscript. Two anonymous reviewers provided additional helpful comments; nevertheless, all errors of interpretation or presentation are ours. We also wish to thank William Hess and the Morton Arboretum for allowing us to sample their hybrid accessions and providing information on the provenance of those hybrids. This research was supported, in part, by Grant DEB 9500499 from the National Science Foundation and by the U. S. Forest Service.

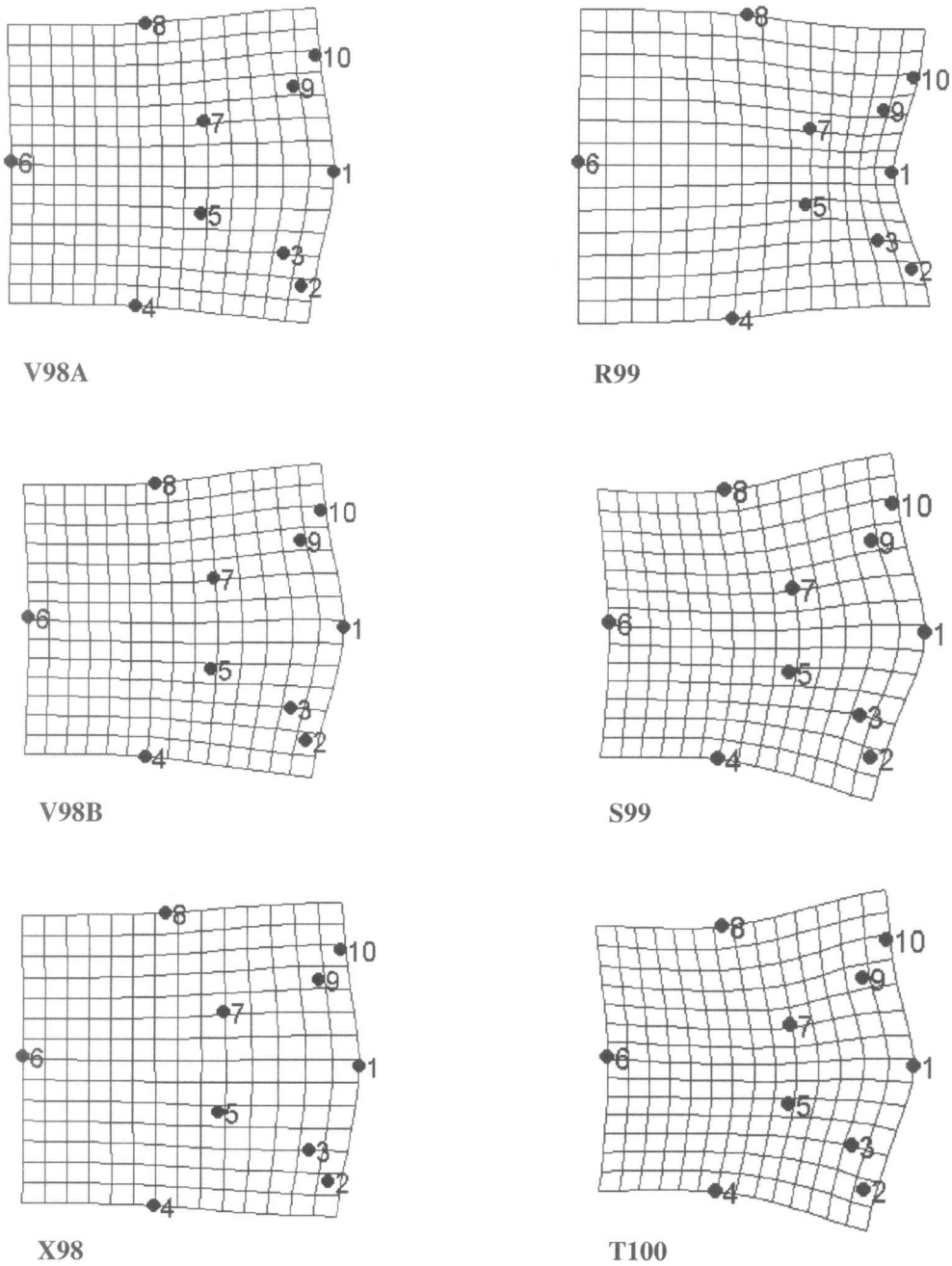

Fig. 11. Relative warps deformation grids for the six hybrid OTUs. Grids oriented with leaf base on the right, leaf apex on the left (compare with Fig. 1).

LITERATURE CITED

Blackith, R. E. 1965. Morphometrics. Pp. 225–249 in: Waterman, T. H. & Morowitz, H. J. (eds.), *Theoretical and Mathematical Biology*. Blaisdell Publishing Co., New York.

Blackith, R. E. & Reyment, R. 1971. *Multivariate Morphometrics.* Academic Press, London.

Bogdanowicz, W. & Owen, R. D. 1996. Landmark-based size and shape analysis in systematics of the plecotine bats. Pp. 489–501 in: Marcus, L. F., Corti, M., Loy, A., Naylor, G. J. P. & Slice, D. E. (eds.), *Advances in Morphometrics.* Plenum Press, New York.

BONAP. 2001. http://www.csdl.tamu.edu/FLORA/cgi/b98map?genus=Acer&species=freemanii.

Bookstein, F. L. 1989. "Size and shape": a comment on semantics. *Syst. Zool.* 38: 173–180.

Bookstein, F. L. 1991. *Morphometric Tools for Landmark Data.* Cambridge Univ. Press, Cambridge.

Bookstein, F. L. 1994. Can biometrical shape be a homologous character? Pp. 197–227 in: Hall, B. K. (ed.), *Homology: the Hierarchical Basis of Comparative Biology.* Academic Press, San Diego.

Bookstein, F. L. 1996. Combining the tools of geometric morphometrics. Pp. 131–151 in: Marcus, L. F., Corti, M., Loy, A., Naylor, G. J. P. & Slice, D. E. (eds.), *Advances in Morphometrics*. Plenum Press, New York.

Bookstein, F. L., Chernoff, B., Elder, R., Humphries, J., Smith, G. & Strauss, R. 1985. *Morphometrics in Evolutionary Biology*. Special Publication 15. The Academy of Natural Sciences of Philadelphia, Philadelphia.

Carpenter, K. E. 1996. Morphometric pattern and feeding mode in emperor fishes (Lethrinidae, Perciformes). Pp. 479–487 in: Marcus, L. F., Corti, M., Loy, A., Naylor, G. J. P. & Slice, D. E. (eds.), *Advances in Morphometrics*. Plenum Press, New York.

Dickinson, T. A., Parker, W. H. & Strauss, R. E. 1987. Another approach to leaf shape comparisons. *Taxon* 36: 1–20.

Elias, T. S. 1980. *The Complete Trees of North America*. Van Nostrand Reinhold Co., New York.

Fernald, M. L. 1970. *Gray's Manual of Botany* (8th ed., corrected printing). Van Nostrand Reinhold Co., New York.

Gelderen, D. M. van, de Jong, P. C. & Oterdoom, H. J. 1994. *Maples of the World*. Timber Press, Portland, Oregon.

Gleason, H. A. 1968. *The New Britton and Brown Illustrated Flora of the Northeastern United States and Adjacent Canada*, 3 vols., ed. 4. Hafner Publishing Co., New York.

Hess, W. J. & Crowley, W. R. 1990. *The Scanning Electron Microscope at Work: Documenting the Parentage of the 'Marmo' Maple*. Morton Arboretum, Lisle, Illinois.

Hickey, L. J. 1973. Classification of the architecture of dicotyledonous leaves. *Amer. J. Bot.* 60: 17–33.

Jensen, R. J. 1988. Assessing patterns of morphological variation of *Quercus* spp. in mixed-oak communities. *Amer. Mid. Nat.* 120: 120–135.

Jensen, R. J. 1990. Detecting shape variation in oak leaf morphology: a comparison of rotational-fit methods. *Amer. J. Bot.* 77: 1279–1293.

Jensen, R. J. 1995. Using leaf shape to identify taxa in a mixed-oak community in Land Between The Lakes, Kentucky. Pp. 177–188 in: Hamilton, S. W., White, D. S., Chester, E. W. & Scott, A. F. (eds.), *Proceedings of the Sixth Symposium on the Natural History of Lower Tennessee and Cumberland River Valleys.* The Center for Field Biology, Austin Peay State Univ., Clarksville, Tennessee.

Jensen, R. J., Hokanson, S. C., Isebrands, J. G. & Hancock, J. F. 1993. Morphometric variation in oaks of the Apostle Islands in Wisconsin: evidence of hybridization between *Quercus rubra* and *Q. ellipsoidalis* (Fagaceae). *Amer. J. Bot.* 80: 1358–1366.

Jensen, R. J., Schwoyer, M., Crawford, D. J., Stuessy, T. F., Anderson, G. J., Baeza, C. A., Silva O., M. & Ruiz, E. In press. Relationships among populations of *Myrceugenia fernandeziana* (Myrtaceae) on Masatierra Island. *Syst. Bot.* 27.

Klingenberg, C. P. & McIntyre, G. S. 1998. Geometric morphometrics of developmental instability: analyzing patterns of fluctuating asymmetry with Procrustes methods. *Evolution* 52: 1363–1375.

Knops, J. F. & Jensen, R. J. 1980. Morphological and phenolic variation in a three species community of red oaks. *Bull. Torr. Bot. Club* 107: 418–428.

Lohmann, G. P. 1983. Eigenshape analysis of microfossils: a general morphometric procedure for describing changes in shape. *Math. Geol.* 15: 659–672.

Mantel, N. A. 1967. The detection of disease clustering and a generalized regression approach. *Cancer Res.* 27: 209–220.

McLellan, T. 1993. The roles of heterochrony and heteroblasty in the diversification of leaf shapes in *Begonia dregei* (Begoniaceae). *Amer. J. Bot.* 80: 796–804.

McLellan, T. & Endler, J. A. 1998. The relative success of some methods for measuring and describing the shape of complex objects. *Syst. Biol.* 47: 264–281.

Meacham, C. A. & Duncan, T. 1991. *MorphoSys*. Regents of the Univ. of California, Berkeley.

Monteiro, L. R. 1999. Multivariate regression models and geometric morphometrics: the search for causal factors in the analysis of shape. *Syst. Biol.* 48: 192–199.

Murray, A. E. 1969. *Acer* Notes nos. 1–6. *Kalmia* 1: 1–42.

Paler, M. H. & Barrington, D. S. 1995. The hybrid *Cystopteris fragilis* × *C. tenuis* (Dryopteridaceae) and the relationship between its tetraploid progenitors. *Syst. Bot.* 20: 528–545.

Premoli, A. C. 1996. Leaf architecture of South American *Nothofagus* (Nothofagaceae) using traditional and new methods in morphometrics. *Bot. J. Linn. Soc.* 121: 25–40.

Ray, T. 1992. Landmark eigenshape analysis: homologous contours: leaf shape in *Syngonium* (Araceae). *Amer. J. Bot.* 79: 69–76.

Rohlf, F. J. 1993a. Relative warp analysis and an example of its application to mosquito wings. Pp. 131–159 in: Marcus, L. F., Bello, E. & Garcia-Valdecasas, A. (eds.), *Contributions to Morphometrics*. Monografías del Museo Nacional de Ciencias Naturales, Madrid.

Rohlf, F. J. 1993b. *NTSYS-pc: Numerical Taxonomy and Multivariate Analysis System (version 1.8).* Applied Biostatistics Inc., New York.

Rohlf, F. J. 2000. *NTSYS-pc: Numerical Taxonomy and Multivariate Analysis System (version 2.1).* Applied Biostatistics Inc., New York.

Rohlf, F. J. 1996. Morphometric spaces, shape components and the effects of linear transformations. Pp. 117–129 in: Marcus, L. F., Corti, M., Loy, A., Naylor, G. J. P. & Slice, D. E. (eds.), *Advances in Morphometrics*. Plenum Press, New York.

Rohlf, F. J. 1997. *TpsRelw. Version 1.16.* Ecology and Evolution, SUNY, Stony Brook, New York.

Rohlf, F. J. 1998. *TpsSmall. Version 1.18.* Ecology and Evolution, SUNY, Stony Brook, New York.

Rohlf, F. J. & Marcus, L. F. 1993. A revolution in morphometrics. *Trends Ecol. Evol.* 8: 129–133.

Rohlf, F. J., Loy, A. & Corti, M. 1996. Morphometric analy-

sis of old world talpidae (Mammalia, Insectivora) using partial warp scores. *Syst. Biol.* 45: 344–362.

Rumpunen, K. & Bartish, I. V. 2002. Comparison of differentiation estimates based on morphometric and molecular data, exemplified by various leaf shape descriptors and RAPDs in the genus *Chaenomeles* (Rosaceae). *Taxon* 51: 69–82.

Slice, D. E., Bookstein, F. L., Marcus, L. F. & Rohlf, F. J. 1996. A glossary for geometric morphometrics. Pp. 531–551 in: Marcus, L. F., Corti, M., Loy, A., Naylor, G. J. P. & Slice, D. E. (eds.), *Advances in Morphometrics.* Plenum Press, New York.

Stace, C. A. 1989. *Plant Taxonomy and Biosystematics*, ed. 2. Cambridge Univ. Press, Cambridge.

Voss, E. G. 1972–1996. *Michigan Flora,* 3 vols. Cranbrook Institute of Science, Bloomfield Hills, Michigan.

White, R. J., Prentice, H. C. & Verwijst, T. 1988. Automated image acquisition and morphometric description. *Can. J. Bot.* 14: 612–623.

Wilson, P. 1992. On inferring hybridity from morphological intermediacy. *Taxon* 41: 11–23.

Woodland, D. W. 1997. *Contemporary Plant Systematics*, ed. 2. Andrews Univ. Press, Berrien Springs, Michigan.